JOURNAL OF CATALYSIS **107**, 140–153 (1987)

Benzene Hydrogenation over Supported and Unsupported Palladium

II. Reaction Model

PEN CHOU AND M. ALBERT VANNICE*

Department of Chemical Engineering, The Pennsylvania State University, University Park, Pennsylvania 16802

Received December 8, 1986; revised April 6, 1987

A modified Langmuir–Hinshelwood (L–H) model has been proposed to describe benzene hydrogenation over both unsupported Pd and supported Pd catalysts. A general reaction sequence proposing sequential addition of H atoms to the benzene ring, with no a priori assumption of a rate-determining step, was used because computer analysis allowed the determination of selected rate and adsorption constants. To explain the observed kinetic behavior, it was necessary to include an auxiliary reaction—benzene dehydrogenation to various carbonaceous surface species—which inhibits the principal reaction. This model, which quantitatively includes hydrogen-deficient species that inhibit the hydrogenation reaction, satisfactorily explains all results that were obtained in this study and is also consistent with other reports in the literature related to isotopic exchange and deactivation reactions. To further evaluate this model, the values of the fitted parameters were analyzed with regard to their physical significance, and they were found to be consistent and within theoretical guidelines imposed by L–H kinetics.

INTRODUCTION

In a previous study kinetic data were reported for benzene hydrogenation over a family of Pd catalysts, and the turnover frequencies based on Pd surface atoms were found to be dependent upon the support and Pd precursor used as well as the pretreatment procedure (*1*). The proposed explanation for this behavior was that additional benzene adsorption sites can be created on certain oxides in the metal–support interfacial region, and hydrogen activated on the Pd can hydrogenate these benzene molecules in addition to those on the Pd surface (*1, 2*). Additional studies suggested that these interfacial sites were less susceptible to inhibition by carbonaceous species formed under reaction conditions than sites on the Pd surface (*1, 2*). Certain aspects of the kinetic behavior were very similar to those reported for benzene hydrogenation over a Ni/SiO_2 catalyst, such as a temperature-dependent maximum in activity and changes in reaction orders with temperature (*3*). Although various kinetic models have been proposed for this reaction, few are applicable over a wide range of reaction conditions. Furthermore, previous models reported in the literature have not quantitatively included an important surface phenomenon which can occur concurrently with this and similar reactions—dehydrogenation of a reactant, in this case benzene, to form surface species which can significantly affect the observed catalytic behavior (*4*). Recently, Paal has reiterated how the interpretation of kinetic data can be complicated by the deposition of carbonaceous species formed under reaction conditions (*5*).

In this paper, the effect of the formation of carbonaceous species under reaction conditions has been incorporated into a rather general reaction sequence which has many similarities to a Langmuir–Hinshelwood model, and it explains quite satisfactorily the kinetic behavior of both sup-

---

* To whom inquires should be sent.

0021-9517/87 $3.00

ported and unsupported Pd catalysts. Although the capability of the model to fit the data well cannot be considered as sufficient proof of its validity, its merits were further evaluated based on its consistency with related surface phenomena and the reasonable values of its kinetic parameters when interpreted in a physical sense.

KINETIC MODEL AND DATA ANALYSIS

Reaction Mechanism

The model proposed cannot be considered exactly as a Langmuir–Hinshelwood (L–H) mechanism because a single rate-determining step (RDS) is not specified; however, it has many similarities to a L–H model because adsorption quasi-equilibrium of reactants is assumed. It is used here to correlate the kinetic data for benzene hydrogenation over Pd catalysts reported in the preceding paper (*2*). The model is derived first for sites only on the Pd surface and is then extended to include additional sites proposed to exist in the metal–support interfacial region. Benzene and hydrogen are assumed to adsorb on different sites on the Pd surface and to exist in quasi-equilibrium with the gas phase. The reaction occurs between associatively adsorbed benzene and dissociatively adsorbed hydrogen, and it proceeds by stepwise addition of hydrogen atoms to the benzene ring. Desorption of cyclohexane is assumed to be fast and irreversible; consequently, the surface concentration of cyclohexane is negligible. A concurrent, *equilibrated,* dehydrogenation reaction sequence involving adsorbed benzene, consistent with recent UHV studies (*6–8*), is included to account for changes in the number of active sites due to inhibition by carbonaceous species formed under different reaction conditions. The proposed model can be described by the following equations (See Appendix A for nomenclature):

$$\mathrm{H}_{2_{(g)}} + 2\mathcal{S} \overset{K_\mathrm{H}}{\longleftrightarrow} 2\mathrm{H}\text{-}\mathcal{S} \qquad (1)$$

$$\mathrm{Bz}_{(g)} + \mathrm{S} \overset{K_\mathrm{B}}{\longleftrightarrow} \mathrm{Bz}\text{-}\mathrm{S} \qquad (2)$$

$$\mathrm{Bz}\text{-}\mathrm{S} + \mathrm{H}\text{-}\mathcal{S} \underset{k_{-1}}{\overset{k_{+1}}{\rightleftharpoons}} B_1\text{-}\mathrm{S} + \mathcal{S} \qquad (3a)$$

$$B_1\text{-}\mathrm{S} + \mathrm{H}\text{-}\mathcal{S} \underset{k_{-2}}{\overset{k_{+2}}{\rightleftharpoons}} B_2\text{-}\mathrm{S} + \mathcal{S} \qquad (3b)$$

$$\cdots \qquad (3c)$$

$$\cdots \qquad (3d)$$

$$\cdots \qquad (3e)$$

$$B_5\text{-}\mathrm{S} + \mathrm{H}\text{-}\mathcal{S} \underset{k_{-6}}{\overset{k_{+6}}{\rightleftharpoons}} \mathrm{C}_6\mathrm{H}_{12_{(g)}} + \mathcal{S} + \mathrm{S} \qquad (3f)$$

$$\mathrm{Bz}\text{-}\mathrm{S} + \mathcal{S} \overset{K_{\mathrm{D}1}}{\longleftrightarrow} D_1\text{-}\mathrm{S} + \mathrm{H}\text{-}\mathcal{S} \qquad (4a)$$

$$\mathrm{Bz}\text{-}\mathrm{S} + 2\mathcal{S} \overset{K_{\mathrm{D}2}}{\longleftrightarrow} D_2\text{-}\mathrm{S} + 2\mathrm{H}\text{-}\mathcal{S} \qquad (4b)$$

$$\cdots \qquad (4c)$$

$$\cdots \qquad (4d)$$

$$\cdots \qquad (4e)$$

$$\mathrm{Bz}\text{-}\mathrm{S} + 6\mathcal{S} \overset{K_{\mathrm{D}6}}{\longleftrightarrow} D_6\text{-}\mathrm{S} + 6\mathrm{H}\text{-}\mathcal{S} \qquad (4f)$$

(An alternate approach to describe these equilibrated dehydrogenation steps would be to express each one as the sequential loss of one H atom; however, the number of independent equations would be the same and the form of the model would remain the same.)

The equilibrium constants for steps (1), (2), and (4a) through (4f) can be expressed in terms of entropy and enthalpy changes as

$$K_i = \exp\left(\frac{\Delta S_i}{R} - \frac{\Delta H_i}{RT}\right), \qquad (5)$$

and each rate constant is defined as

$$k_i = N_s\left(\frac{kT}{h}\right)\exp\left(\frac{\Delta S_i^*}{R} - \frac{\Delta H_i^*}{RT}\right) = Ae^{-E/RT}, \qquad (6)$$

where N_s, ΔS_i^*, ΔH_i^* are site density, entropy of activation, and enthalpy of activation, and k, h, and R are the Boltzmann, Planck, and gas constants, respectively.

This reaction has been previously studied over Ni catalysts, and there is much similarity in the kinetic behavior over Ni and Pd; therefore, some assumptions in our proposed model are based on results reported for Ni catalysts. Studies indicate that preadsorbed hydrogen does not prevent the chemisorption of benzene, and benzene chemisorption on metals is limited to only partial coverage of the metal surface (*9–12*). The first observation suggests that benzene is likely to preferentially adsorb on the more energetic sites under reaction conditions. Considering the size of the benzene molecule (Van der Waals radius = 3.40 Å), it is not unexpected that steric constraints can provide gaps allowing hydrogen access to adsorption sites not accessible to adsorbing benzene; for example, the hollow sites that exist between metal atoms on surfaces of threefold and fourfold symmetry (*13*). Although hydrogen may compete with benzene for a portion of the surface, several studies suggest that weakly adsorbed hydrogen is the main form involved in this hydrogenation reaction (*12, 14, 15*). Using magnetization measurements, van Meerten *et al.* have shown that this weakly adsorbed hydrogen is indeed dissociatively adsorbed (*14*). In addition, a recent study by Mirodatos has shown that surface coverage of hydrogen can be quite high in the presence of adsorbed benzene (*16*). On the basis of these results, the designation of a different site for hydrogen adsorption is quite reasonable and seems justified.

A rate-determining step is not specified in this reaction sequence because there may not be one and, even if there is, this RDS may change over a wide range of reaction conditions. The stepwise addition of a hydrogen atom, which involves only a bimolecular surface reaction, was chosen because this reaction probability is higher than that for simultaneous multiple additions of hydrogen atoms. Another assumption regarding the hydrogenation process is the favorable desorption of the final product, C_6H_{12}. Chemisorption of saturated hydrocarbons on metals like Pd is through a process of breaking a C–H bond and forming a σ-bond with the metal (*17*). Since the last hydrogenation step destroys the σ-bond, desorption of cyclohexane is expected to occur very easily and surface concentrations of cyclohexane are negligible. Although studies have found measureable uptakes of hydrocarbon when Ni is exposed to cyclohexane, these strongly adsorbed species are most likely dehydrogenated cyclohexane species (*10*). Also, adsorbed hydrogen inhibits the rupture of C–H bonds and strongly affects the adsorption of cyclohexane on Ni up to 448 K (*10*).

There is strong evidence suggesting that some dehydrogenation occurs during the adsorption of benzene on Group VIII metals, especially at higher temperatures and in the absence of hydrogen, as discussed later. In fact, because of the easy access of the metal to the π electrons, the benzene molecule is readily perturbed and the rupture of C–H bonds is probably much more feasible than with saturated hydrocarbons. The removal of these dehydrogenated species from the Pd surface by a treatment in hydrogen implies that the dehydrogenation reactions are reversible (*2*). The consequence of this dehydrogenation process is a reduction in the number of active sites available for the hydrogenation reaction, the extent of which depends on reaction conditions, and the inclusion of these hydrogen-deficient species in the kinetic model is needed to describe the observed kinetic behavior. This sequence is represented by six parallel steps, which are assumed to be in equilibrium with adsorbed benzene under steady-state reaction conditions because none of these hydrogen-deficient species is expected to desorb directly from the catalyst.

Using the steady-state approximation for steps (3a) through (3f) and assuming step (3f) is irreversible, the rate of benzene hydrogenation can be expressed as

$$r(\mu\text{mole Bz} \cdot \text{s}^{-1} \cdot \text{g-cat}^{-1}) = k_{+6}\Theta_{B_5}\Theta_H. \quad (7)$$

As shown in Appendix B, expressions for Θ_{B_1} to Θ_{B_5} can be derived and related to Θ_{Bz} and Θ_H through rate constants and equilibrium constants, where $\Theta_{Bz} = K_B P_B \Theta_S$ and $\Theta_H = (K_H P_H)^{1/2}\ \Theta_{\mathscr{S}} = (K_H P_H)^{1/2}/(1 +$

$(K_HP_H)^{1/2}$). Similarly, by using steps (4a) through (4f), Θ_{D_1} to Θ_{D_6} can be related to Θ_{Bz} and Θ_H through their equilibrium constants (Appendix B). Then by employing conservation of S-type sites,

$$\Theta_S + \Theta_{Bz} + \Theta_{D_1} + \ldots + \Theta_{D_6} + \Theta_{B_1} + \ldots + \Theta_{B_5} = 1, \quad (8)$$

one can express all these surface coverages in terms of P_H, P_B, rate constants k_i, and equilibrium constants K_{D_i}. The similarity of the final form to a Langmuir expression is apparent:

$$r = k_{+6}\left(\frac{(K_HP_H)^{1/2}}{1 + (K_HP_H)^{1/2}}\right)\left(\frac{C_8K_BP_B}{1 + K_BP_B(1 + \Sigma_iX_i + \Sigma_iY_i)}\right). \quad (9)$$

The terms representing C_8, X_i, and Y_i are rather complex, as shown in Appendix B, but they can readily be determined using a computer.

Following the concept of adlineation, first described by Schwab (*18*), it has been proposed for supported Pd catalysts that the region at the metal–support interface can provide additional adsorption sites for benzene and thereby enhance the activity (*1*). The much lower specific activity, expressed as a turnover frequency (TOF = Bz molecule $\cdot$ s^{-1} $\cdot$ Pd_s^{-1}), of unsupported Pd compared to TOF values for supported Pd catalysts suggests that sites on the Pd surface may provide only a small contribution to the overall activities measured for Pd dispersed on certain metal oxides. Therefore, these interfacial sites may be extremely important in specific reactions. Since the dehydrogenation of aromatic hydrocarbons can also occur on oxides, this model for Pd is presumed to also be applicable to these interfacial sites. However, these oxides do not activate hydrogen under the reaction conditions used here; consequently, the only source of activated hydrogen is from the Pd crystallites. Under appropriate conditions the migration of hydrogen atoms from the metal phase onto an oxide cannot only be fast but also be assisted by aromatic hydrocarbons (*19–21*). In addition, we presume that these hydrogen atoms must migrate for only very short distances on the support before they react with benzene (*1, 2*). Therefore, the surface concentration of activated hydrogen in this metal–support interfacial region is assumed to be in quasi-equilibrium with that on the Pd crystallites, i.e.,

$$\text{H-}\mathcal{S} \overset{K_{(\mathcal{S})}}{\longleftrightarrow} \text{H}_s \quad (10)$$

where H_s is hydrogen on the support surface. This concentration of hydrogen atoms on the support $[H_s]$, will then have the same form as that on the Pd surface; i.e.,

$$[H_s] = \frac{(K'_HP_H)^{1/2}}{1 + (K'_HP_H)^{1/2}}, \quad (11)$$

and all the equations describing benzene adsorption and reaction on the interfacial sites have the same form as those derived for sites on the Pd surface itself. Consequently, we have two parallel reaction paths, each with the same form of the rate equation but with slightly different interpretations of the constants.

Data-Fitting Procedure

Benzene conversions were kept below 10% to avoid heat and mass transfer effects by using at least three different sample sizes to cover the range of reaction conditions studied (340–573 K, 300–700 Torr H_2 and 30–70 Torr benzene). Since the activities measured for different samples of the same catalyst did not always match exactly, presumably because of small differences in Pd dispersion, not all the raw data (i.e., measured activities) were used directly in data fitting. Apparent activation energies derived from rates measured in the low-temperature region below 423 K and reaction orders derived from partial pressure dependency data were used in the data-fitting process (*2*), and the activity data measured in the higher temperature region where curvature and a temperature-dependent maximum occurred were used to quantify specific activity.

The simplex method of Nelder and Mead was used on a Digital VAX 11/780 computer to obtain the rate constants and the equilibrium constants which gave optimum fitting (*22*). To reduce the number of adjustable parameters and the computation time, only K_{D_1} and K_{D_6} were considered as independent constants in the benzene dehydrogenation process, and each of these contains two adjustable parameters, i.e., the entropy and enthalpy changes. The values of ΔS_i and ΔH_i for K_{D_2} to K_{D_5} were assumed to be linearly distributed between those of K_{D_1} and K_{D_6}; for example, $\Delta S_{D_3} = \Delta S_{D_1} + 2(\Delta S_{D_6} - \Delta S_{D_1})/5$. A similar approach was taken with ΔS_i^* and ΔH_i^* to determine the rate constants k_{+2} to k_{+5} and k_{-2} to k_{-5}, and only k_{+1}, k_{+6}, k_{-1}, and k_{-6} were considered as independent constants. This more complex model including inhibition by C_6H_{6-i} (D_i) species was required to describe all the essential catalytic phenomena, and because of the range of temperature and pressure over which the data were gathered, we decided to utilize the computer to obtain as much information as possible about the surface species present, based on our assumptions. We are the first to concede that the predicted concentrations should not be interpreted rigorously, but their relative values and trends with reaction conditions should be instructive. Data collected at temperatures below 380 K contained limited information because most of the measured kinetic parameters, such as apparent activation energy and reaction orders, changed little, but at higher temperatures many kinetic parameters became quite temperature sensitive and experimental data provided a more stringent test for the proposed model. Unfortunately, the highest temperature in the experiments was limited by the equilibrium conversion for benzene hydrogenation, as it decreases sharply above 590 K at the reaction conditions employed (*2*).

RESULTS

Our previous study showed that benzene hydrogenation on unsupported Pd powder has different kinetic behavior compared to that observed for supported Pd catalysts (*2*). Since the kinetic parameters for this reaction on all the supported catalysts were almost identical, with the exception of turnover frequencies, a 1.80% Pd/Al_2O_3 sample was chosen as a representative catalyst, examined in detail, and compared with the Pd powder. A problem with modeling when a data-fitting approach such as this is utilized is that the parameters obtained may retain no physical meaning related to the process they describe, and the final values for these parameters may depend on the initial guess and not represent unique values. The same difficulty has also been recognized by other investigators using models containing a smaller number of parameters (*23*); however, no a priori constraints were imposed to obtain the parameters reported here. Although some uncertainty about their uniqueness may exist, a wide range of initial guesses typically resulted in convergence to final parameter values which agreed to within ±15%. Two of the most different sets of such values for each catalyst are listed in Table 1. The similarity between most values in the two sets is apparent, and the differences could easily represent the uncertainty associated with each parameter value due to experimental error.

The results using only one set of parameters for each catalyst are plotted in Figs. 1 and 2 because for a given set (I or II) similar plots were obtained for either catalyst (*24*). The apparent activation energies measured at low temperatures were obtained from the plots given in the preceding paper (*2*), and the actual data points are therefore not shown in Figs. 1 and 2. The coverages of different surface species calculated from the model are plotted in Figs. 3 and 4. It

TABLE 1

Derived Parameters for the Benzene Hydrogenation Model

Catalyst	K_H	K_B	K_{D_1}	K_{D_6}	k_{+1}	k_{-1}	k_{+6}	E_a (kcal $mole^{-1}$)[a]	
								Measured	Calculated
Pd/Al_2O_3[b]									
Set I									
ΔS, ln A	−15.3	−34.2	−10.1	48.3	14.3	15.9	15.9	12.4	12.4
ΔH, ΔH^*	−1.8	−19.7	−0.6	48.1	6.5	9.6	5.7		
Set II									
ΔS, ln A	−13.8	−33.4	−3.6	46.3	15.0	17.9	15.8	12.4	12.4
ΔH, ΔH^*	−1.4	−18.0	0.0	44.5	6.5	10.3	6.2		
Pd powder[b]									
Set I									
ΔS, ln A	−16.5	−24.4	−5.6	32.2	11.2	12.9	12.3	12.9	12.9
ΔH, ΔH^*	−1.5	−14.0	1.4	36.7	6.8	9.5	5.6		
Set II									
ΔS, ln A	−15.5	−31.2	−3.7	45.1	11.8	13.6	13.8	12.9	12.9
ΔH, ΔH^*	−1.4	−16.9	0.3	42.4	6.8	9.6	6.7		

[a] Apparent activation energy at temperatures below 413 K.

[b] For rate constants, $\ln A = \ln(N_s kT/h) + \Delta S^*/R_0$ (see Nomenclature, Appendix A).

was here that the largest differences were observed as a result of variations in the constants which govern the relative coverages of benzene and the dehydrogenated species, especially for the K_{D_1} values.

DISCUSSION

Some discussion is warranted regarding the inclusion of a dehydrogenation sequence to form surface species which inhibit the reaction rate. Angle-resolved photoemission spectra have indicated that benzene is adsorbed on Pd through a π-bonding interaction with the metal which orients the ring parallel to the surface (*25*). Electron energy loss spectra have also suggested that the hydrogen atoms in benzene interact with metal substrates (*26, 27*). Such interactions can lead to rupture of the C–H bond and produce gas phase hydrogen and surface carbon during thermal desorption of benzene from Pd surfaces (*6, 7*). In fact, earlier studies had shown that rupture of the C–H bond occurs during the chemisorption of benzene on some Group VIII metals (*28, 29*). A certain extent of benzene dehydrogenation is also implied by studies based on magnetization measurements (*30, 31*) and H–D exchange between C_6H_6 and C_6D_6 (*32*), as discussed elsewhere (*2*). In at least one study, the hydrogen produced from this dehydrogenation step was reported to react with benzene to form cyclohexane (*33*). Benzene adsorbed on oxides may undergo similar dehydrogenation steps, as suggested by isotopic exchange between C_6H_6 and C_6D_6 (*34*) and coke formation on cracking catalysts. Studies by Sinfelt and co-workers of reforming reactions such as dehydrocyclization have shown the large positive effect H_2 pressure can have on activity and maintenance, thus supporting the postulate that hydrogen-deficient species are formed (*35, 36*). Therefore, depending on the ambient H_2 pressure, adsorbed benzene may either react with hydrogen or lose hydrogen, but the desorption of these dehydrogenated species from the catalyst surface has not been observed and they will eventually equilibrate with adsorbed benzene and hydrogen.

To further evaluate this model, the physi-

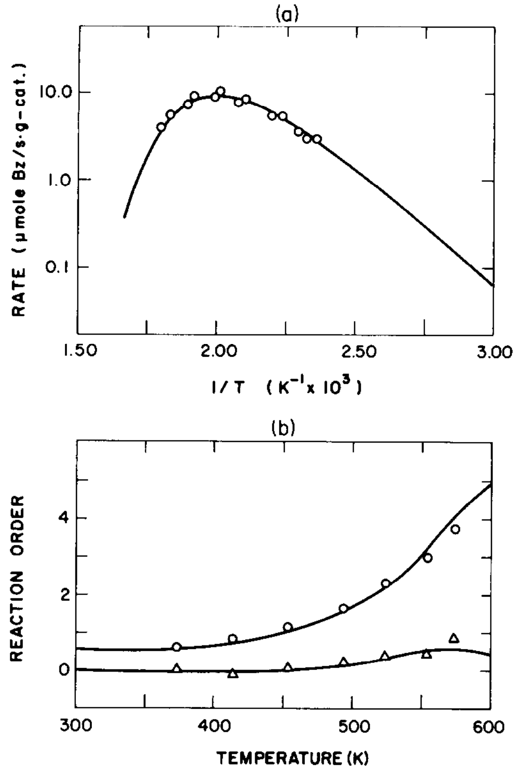

FIG. 1. (a) Activity for benzene hydrogenation over 1.8% Pd/Al_2O_3 at 50 Torr benzene and 680 Torr hydrogen: O–experimental data; solid line calculated by using parameters from Set I (Table 1). (b) Activity for benzene hydrogenation on 1.8% Pd/Al_2O_3: O–reaction order in hydrogen, Δ–reaction order in benzene; solid lines calculated using parameters from Set 1.

cal significance of the parameters in Table 1 was analyzed. For benzene, the calculated heats of adsorption ($Q_B = -\Delta H_B$) on the Pd powder of 14–17 kcal/mole are quite reasonable compared to values reported for Ni—25 kcal $mole^{-1}$ for a clean surface and 10 kcal $mole^{-1}$ at near-monolayer coverage (*37*)—and they imply that the reactive benzene is not too strongly adsorbed. This seems plausible because the species interacting most strongly with the catalyst would be most likely to undergo dehydrogenation to form inert species. For the supported catalyst, the $-\Delta H_B$ values are somewhat higher and are comparable to the values of 12–18 kcal $mole^{-1}$ reported for benzene adsorption on SiO_2, SiO_2–Al_2O_3, and zeolites (*38, 39*). Van Meerten *et al.* have estimated that the entropy changes for benzene adsorption (ΔS_B) are −33 and −47 e.u. (1 e.u. = 1 cal $mole^{-1}$ K^{-1}) for mobile and immobile species, respectively (*23*). Based on these estimations, the ΔS_B values in Table 1 are also very reasonable and they imply that the benzene species involved in the reaction are relatively mobile, which is consistent with the conclusion of Primet *et al.* based on IR studies (*40*) and a recent isotopic transient study by Mirodates (*16*).

The entropy change for hydrogen adsorption is consistent with that expected for dissociative adsorption (*41*); however, the heat of adsorption ($Q_H = -\Delta H_H$) is much

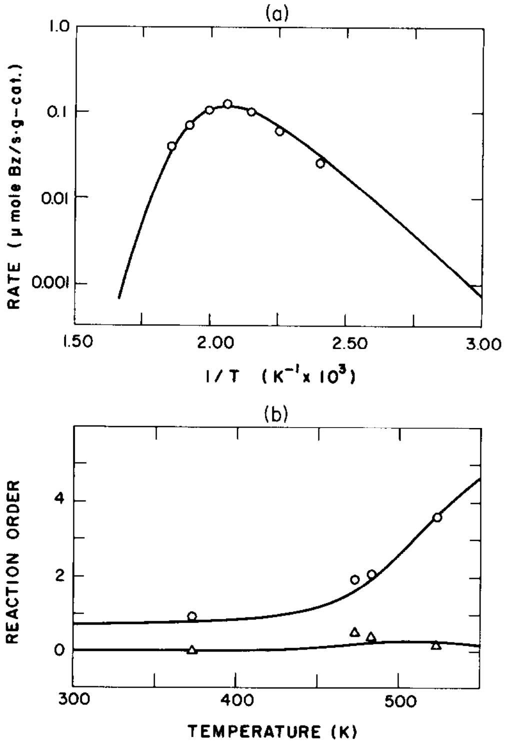

FIG. 2. (a) Activity for benzene hydrogenation over Pd powder at 50 Torr benzene and 680 Torr hydrogen: O–experimental data; solid line calculated using parameters from Set II (Table 1). (b) Reaction orders for benzene hydrogenation over Pd powder: O–reaction order in hydrogen, Δ–reaction order in benzene; solid line calculated by using parameters from Set II.

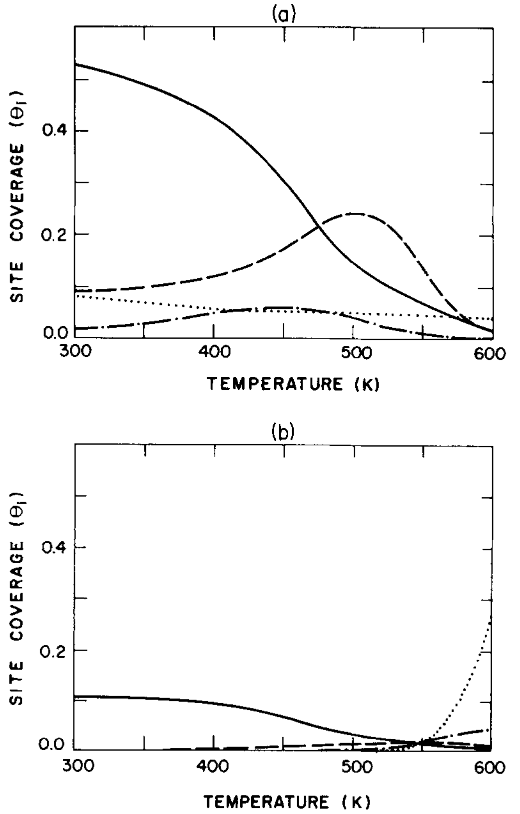

FIG. 3. Coverages of surface species on 1.8% Pd/Al_2O_3 under reaction conditions at 50 Torr benzene and 680 Torr hydrogen calculated from the model using parameters from Set I: (a) Θ_H: ···; Θ_{Bz}: —; Θ_{B_2}: ---; Θ_{B_4}: -·-. (b) Θ_{D_1}: —; Θ_{D_2}: ---; Θ_{D_4}: -·-; Θ_{D_6}: ···.

lower than the integral heats of adsorption (15 kcal mole^{-1}) measured on these samples (*42*). There are various possible explanations for this. Since benzene is preferentially adsorbed, the sites remaining for hydrogen provide only weak bonding. In addition, the $-\Delta H_H$ values obtained from the kinetic data reflect only the hydrogen participating in the reaction and could be significantly different from heats of adsorption measured calorimetrically on a clean Pd surface at lower temperatures. In several studies it has been reported that hydrogen adsorbed at low coverages does not react with benzene, and the reaction begins only when the surface is nearly saturated and contains weakly adsorbed hydrogen (*12, 14, 15, 43*). Since the hydrogenation reaction also involves the rupture of Pd–H bonds, a higher activity for weakly adsorbed hydrogen atoms is not surprising. This conclusion is further justified by our model because at low hydrogen surface coverages, steps (4a) through (4f) show that the conversion of benzene to inactive species is favored. It should be pointed out that although Figs. 3 and 4 indicate rather low hydrogen coverages at almost all reaction conditions, these coverages pertain only to those adsorption sites involved in the reaction. Additional forms of adsorbed hydrogen, not involved in the reaction, could also exist.

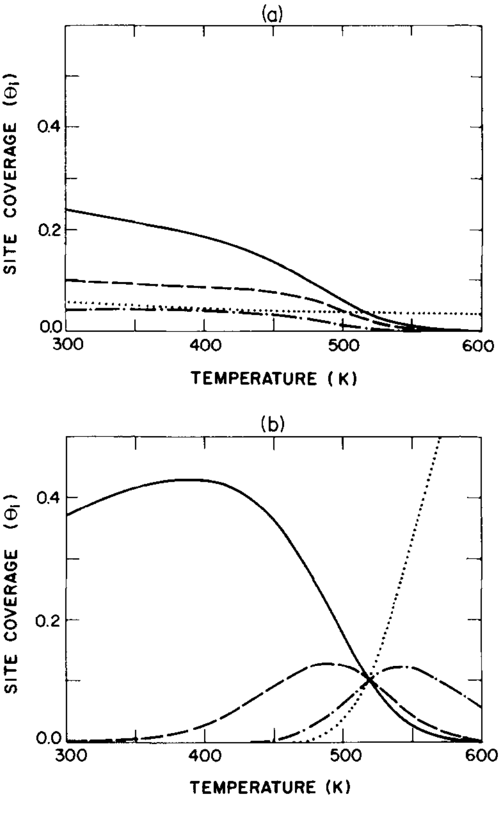

FIG. 4. Coverages of surface species on Pd powder under reaction conditions at 50 Torr benzene and 680 Torr hydrogen calculated using parameters from Set II: (a) Θ_H: ···; Θ_{Bz}: —; Θ_{B_2}: ---; Θ_{B_4}: -·-. (b) Θ_{D_1}: —; Θ_{D_2}: ---; Θ_{D_4}: -·-; Θ_{D_6}: ···.

For either catalyst, the parameters from Set I predict different surface concentration profiles from those obtained using parameters in Set II; that is, the former predict mild dehydration and relatively high benzene coverages whereas the latter imply more severe benzene dehydrogenation and much lower benzene coverages. However, both illustrate the sharp decline in Θ_{Bz} around 500 K that results in the activity maximum observed for all catalysts, as described previously for this reaction over iron catalysts (*44*). An example of each set is given in Figs. 3 and 4. The principal difference is an inversion of the ratio of adsorbed benzene to dehydrogenated benzene. Although it is difficult to pick the more representative case based only on the parameter values, benzene dehydrogenation at higher temperatures (as indicated by Θ_{D_6}) is clearly much more severe on unsupported Pd than on the supported catalyst. This is consistent with the experimental results that showed more inhibition occurred on Pd powder (*2*), and it suggests that the set of parameters (II) predicting severe dehydrogenation is more appropriate for unsupported Pd while Set I is more applicable to the supported Pd catalysts. Therefore, one difference in kinetic behavior between supported and unsupported Pd catalysts may be that sites on Pd are more susceptible to inhibition by carbonaceous species than sites in the metal–support interfacial region (*2*).

An interesting aspect of this model is that it also can describe the isotope exchange reaction between deuterium and benzene, which has been explained in terms of either an associative or a dissociative mechanism (*4, 32*), with the former corresponding to steps (3a) to (3e) and the latter to steps (4a) to (4f). One difficulty with the associative mechanism has been that many studies have indicated that the exchange and the hydrogenation reactions of benzene proceed through different routes (*45, 46*), but the incorporation of dehydrogenation into the model resolves this problem because the exchange and the hydrogenation reactions are decoupled.

The parameters in Table 1 indicate that dehydrogenation of adsorbed benzene is an endothermic process, in agreement with thermodynamic data, and would be favored at higher temperatures. It should be noted that thermodynamic heats of formation of benzene in most references are based on graphite, but dehydrogenation of benzene only to a carbon ring is assumed here. The entropy change of this process (ΔS_{D_i}) includes a gain from the additional freedom of detached hydrogen atoms and a loss due to the decreased mobility of the carbon ring; consequently, ΔS_{D_i} can be either negative or positive for the loss of the first H atom but the loss of additional H atoms from the benzene molecule causes ΔS_{D_i} to become more positive. The model predicts lower surface concentrations of C_6H_{6+i} (B_i) species than for benzene itself in the low-temperature range, but on supported Pd these concentrations appear to reach a maximum and may even exceed Θ_{Bz} at higher temperatures (see Fig. 3). This predicted result is consistent with experimental evidence that cyclohexene was detected during benzene hydrogenation over a Ni/SiO_2 catalyst when the temperature was raised above 427 K (*47*).

The uncertainty in the rate constants obtained from curve fitting is probably greater than that for the other parameters because steps (3a) to (3e) are assumed to be reversible, and different combinations of k_{+i} and k_{-i} may give almost equally good fits of the data. Nevertheless, the rate constant parameters in Table 1 are reasonable when analyzed. The values of ΔH^* for the reaction between an adsorbed hydrogen atom and $C_6H_{6(ad)}$ or $C_6H_{11(ad)}$ lie between 11 and 14 kcal mole^{-1}, which is near the lower limit for most reactions between two molecules and the upper limit for reactions between a radical and a molecule (*48*).

The preexponential factors in the rate constants are more difficult to evaluate because their magnitude is determined by both site density and entropies of activation, ΔS^*. Since an adsorbed hydrogen atom is combined with the benzene ring, some entropy decrease is anticipated during the formation of the activated complex. On the other hand, the C_6H_{6+i} species formed may simultaneously gain a certain amount of freedom because the bonding strength between it and the catalyst should decrease as the carbon ring becomes more saturated with hydrogen. A quantitative estimation of ΔS^* requires a detailed knowledge of the activated complex, but a very approximate estimate can be made by assuming the entropy loss for a hydrogen atom is that associated with a change from a two-dimensional gas to immobile adsorption, i.e., about 10 e.u. (*41*). Based on this value and the derived rate expression (Eq. (9) plus Eq. (6)), calculated active site densities were two to three orders of magnitude lower than the number of surface Pd atoms (Pd_s). This is remarkably consistent with an active site density of less than 1% of the surface Ni atoms reported by Mirodatos (*16*). This may reflect the coverage of many Pd_s atoms (up to 7, for example) by each benzene molecule as well as the coverage of sites by the inactive dehydrogenated species. For neither catalyst was the estimated number of active sites greater than the number of Pd_s atoms.

Isotope effects in this reaction have already been examined, and considering only their influence on the rate constant, van Meerten *et al.* have stated that hydrogenation of benzene should be faster than deuteration; however, they found no isotope effect at 358 K (*46*). In another study the reaction at 513 K was found to be more rapid when deuterium was present in either reactant (*49*). These studies also found that isotopic exchange between the two reactants was fast, and exchange between C_6H_6 and D_2 was reported to be much faster than between C_6D_6 and H_2. If the isotope effects observed for the exchange reaction can be associated with the tendency of benzene (C_6H_6 or C_6D_6) to undergo dehydrogenation (via the dissociative mechanism of isotope exchange), an explanation for the difference in these two studies can be proposed from our model. Since the exchange reaction is fast, the discussion will focus on hydrogenation of C_6H_6 by H_2 and deuteration of C_6D_6 by D_2. The isotopic exchange studies suggest that the C–D bonds in the aromatic ring have less tendency to rupture than the C–H bonds; therefore, catalysts are less inhibited by deposition of carbonaceous species when C_6D_6 is used. However, at low temperatures where inhibition by formation of dehydrogenated species is not too serious, this advantage may be neutralized by the smaller rate constant for deuteration of C_6D_6 compared to hydrogenation of C_6H_6. At higher temperatures dehydrogenation is more severe, and the greater resistance of C_6D_6 would leave more active sites than C_6H_6, which could more than compensate for the smaller rate constant for deuteration compared to hydrogenation. The isotope effect would then be opposite to that predicted based only on the hydrogenation/deuteration rate constant.

Although the model proposed in this paper is consistent with many experimental studies and more comprehensive than previous models, it still does not include the possibility that benzene dehydrogenation may lead to other reactions, such as hydrogenolysis, and smaller hydrocarbon fragments have indeed been reported (*33, 47, 50*). Other limitations tend to be intrinsic to all L–H-type models; for example, only one type of site was assumed for hydrogen, but those sites involved in the dehydrogenation steps may be different from those involved in the hydrogenation steps. Although it may be possible to further modify this model to better describe the surface phenomena associated with this reaction, it would add even more parameters. In addition, it has been shown that more complicated models invoking surface heterogeneity frequently give rate expressions very similar to more idealized models (*51*). The model proposed here is consistent and correlates the experimental results very well, as admittedly it should with the number of adjustable parameters involved. If one takes the liberty to assume its validity and gives physical meaning to the fitting parameters, the entropy and enthalpy values are quite consistent with theoretical estimates. Consequently, at the very least, this model is certainly plausible and cannot be automatically rejected because of meaningless constants. In addition, it provides a predictive capability that can be used in future studies to test it more completely.

SUMMARY

The kinetic behavior observed for benzene hydrogenation over a Pd/Al_2O_3 catalyst and unsupported Pd powder has been described by a reaction model for benzene hydrogenation that includes a reversible dehydrogenation process for adsorbed benzene which inhibits the reaction rate. Numerous studies reported in the literature have strongly suggested that this dehydrogenation process may occur under reaction conditions, and the carbonaceous species formed are presumed to occupy reaction sites and to thereby decrease activity. Although this model has not been definitively proven, it does explain the kinetic behavior observed for benzene hydrogenation, it is very consistent with other related surface processes reported in the literature, and it has parameter values which are consistent with a physical interpretation based on L–H kinetics. The model indicates that it is the weakly adsorbed hydrogen and benzene that are the principal reactants and that sites on the Pd surface have a greater tendency to be deactivated by carbonaceous species formed from benzene dehydrogenation than sites proposed to exist on the support in the metal–support interfacial region. Most importantly, this study has demonstrated that when deriving a kinetic model for a specific reaction, all related surface phenomena, including those not directly involved in the reaction mechanism, should be examined in order to obtain the most consistent interpretation of the observed kinetic data.

ACKNOWLEDGMENT

This study was funded by the U.S. DOE, Division of Basic Energy Sciences, under Grant DD-FS02-84ER13276.

APPENDIX A

NOMENCLATURE

A	Preexponential factor
B_i	Hydrogenated benzene surface species, $i = 1, \ldots, 6$. $B_1 = C_6H_7$, $B_2 = C_6H_8$, etc.
D_i	Dehydrogenated benzene surface species, $i = 1, \ldots, 6$. $D_1 = C_6H_5$, $D_2 = C_6H_4$, etc.
E	Apparent activation energy
ΔH_i	Standard enthalpy change (K cal mole^{-1})
ΔH_i^*	Enthalpy of activation, $i = -6, \ldots, -1, +1, \ldots, +6$ (K cal mole^{-1})
$[H_s]$	Hydrogen concentration on support
h	Planck constant (6.6262×10^{-27} erg s)
K_B	Equilibrium constant for benzene adsorption on Pd
K_{D_i}	Equilibrium constant for benzene dehydrogenation steps
K_H	Equilibrium constant for hydrogen adsorption on Pd
K_H'	Equilibrium constant for hydrogen adsorption on support
k_i	Rate constant (μmole Bz s^{-1} g^{-1}). Forward steps: $i = +1, \ldots, +6$; reverse steps: $i = -1, \ldots, -6$
k	Boltzmann constant (1.38×10^{-16} erg K^{-1})
N_s	Site density (μmole g^{-1})
P_B	Benzene pressure (atm)
P_H	Hydrogen pressure (atm)
R	Gas constant (1.987 cal mole^{-1} K^{-1})
r	Reaction rate (μmole Bz s^{-1} g^{-1})

S	Hydrocarbon adsorption site on Pd (or support)
$\mathcal{S}$	Hydrogen adsorption site on Pd
ΔS	Standard entropy change (cal mole^{-1} K^{-1})
ΔS_i^*	Entropy of activation, $i = -6, \ldots, -1, +1, \ldots, +6$ (cal mole^{-1} K^{-1})
T	Temperature (K)
Θ_i	Fraction of site coverage by species i on Pd
Θ_S, $\Theta_{\mathcal{S}}$	Fraction of vacant sites on Pd for hydrocarbons and H, respectively

APPENDIX B

Derivation of the Benzene Hydrogenation Reaction Mechanism

Under steady-state conditions when step (3f) is irreversible, the rate of benzene hydrogenation can be expressed as

$$r(\mu\text{mole Bz/s}\cdot\text{g-cat}) = k_{+6}\Theta_{B_5}\Theta_H, \quad (B.1)$$

The coverages of surface species are

$$\Theta_{Bz} = K_B P_B \Theta_S, \quad (B.2)$$

$$\Theta_H = \frac{A}{1+A}, \text{ where } A = (K_H P_H)^{1/2}, \quad (B.3)$$

$$\Theta_{D_1} = \frac{K_{D_1}}{A} K_B P_B \Theta_S, \quad (B.4)$$

. . .

$$\Theta_{D_i} = \frac{K_{D_i}}{A} K_B P_B \Theta_S, \quad (B.5)$$

. . .

$$\Theta_{D_6} = \frac{K_{D_6}}{A} K_B P_B \Theta_S, \quad (B.6)$$

$$\Theta_{B_1} = \frac{C_4C_8}{C_5} K_B P_B \Theta_S, \quad (B.7)$$

$$\Theta_{B_2} = C_9 K_B P_B \Theta_S, \quad (B.8)$$

$$\Theta_{B_3} = \frac{C_8}{C_1} K_B P_B \Theta_S, \quad (B.9)$$

$$\Theta_{B_4} = C_{10} K_B P_B \Theta_S, \quad (B.10)$$

and

$$\Theta_{B_5} = C_8 K_B P_B \Theta_S, \quad (B.11)$$

$$C_1 = \frac{k_{+5}k_{+4}A^2}{(k_{-5} + k_{+6}A)(k_{-4} + k_{+5}A) - k_{-5}k_{+5}A}, \quad (B.12)$$

$$C_2 = \frac{k_{-3} + k_{+4}A}{k_{-4}} - \frac{k_{+4}A}{k_{-4} + k_{+5}A}, \quad (B.13)$$

$$C_3 = \frac{k_{-2} + k_{+3}A}{k_{-3}} - \frac{k_{+3}A}{C_2k_{-4}}, \quad (B.14)$$

$$C_4 = \frac{C_2}{C_1} - \left(\frac{k_{+3}A}{k_{-4}C_2C_3} + 1\right)\frac{k_{-5}}{k_{-4} + k_{+5}A}, \quad (B.15)$$

$$C_5 = \frac{k_{+3}k_{+2}A^2}{C_3k_{-4}k_{-3}}, \quad (B.16)$$

$$C_6 = \frac{k_{-1} + k_{+2}A}{k_{-2}} - \frac{k_{+2}A}{C_3k_{-3}}, \quad (B.17)$$

$$C_7 = \frac{C_5k_{-5}}{C_2C_3C_4C_6(k_{-4} + k_{+5}A)}, \quad (B.18)$$

$$C_8 = \frac{C_5k_{+1}A}{C_4C_6k_{-2}(1 - C_7)}, \quad (B.19)$$

$$C_9 = \frac{C_4C_8k_{+2}A}{C_5(k_{-2} + k_{-3}A)} + \frac{C_8k_{-3}}{C_1(k_{-2} + k_{+3}A)}, \quad (B.20)$$

$$C_{10} = \frac{C_8k_{+4}A + C_1C_8k_{-5}}{C_1(k_{-4} + k_{+5}A)}. \quad (B.21)$$

The expressions for Θ_{D_i} and Θ_{B_i} in Eq. (B.4) through (B.11) can be rewritten as $\Theta_{D_i} = X_iK_BP_B\Theta_S$ and $\Theta_{B_i} = Y_iK_BP_B\Theta_S$, respectively, where $X_i = K_{D_i}/A$, $Y_1 = C_4C_8/C_5$, $Y_2 = C_9$, $Y_3 = C_8/C_1$, $Y_4 = C_{10}$, and $Y_5 = C_8$. After substituting the coverages of all the hydrocarbon species into Eq. (B.7) and solving for Θ_S, one obtains

$$\Theta_S = \frac{1}{1 + K_B P_B(1 + X_1 + \cdot\cdot\cdot + X_6 + Y_1 + \cdot\cdot\cdot + Y_5)}. \tag{B.22}$$

By substituting Θ_S into Eq. (B.4) through (B.11), one can express the coverages of all the surface carbonaceous species in terms of rate constants, equilibrium constants, and partial pressures of benzene and hydrogen. Using Eq. (6) the reaction rate (Eq. (B.1) then becomes

$$r = N_s \left(\frac{kT}{h}\right) \exp\left(\frac{\Delta S^{\ddagger}_{6}}{R} - \frac{\Delta H^{\ddagger}_{6}}{RT}\right)\left(\frac{(K_H P_H)^{1/2}}{1 + (K_H P_H)^{1/2}}\right) \left(\frac{C_8 K_B P_B}{1 + K_B P_B(1 + X_1 + \cdot\cdot\cdot + X_6 + Y_1 + \cdot\cdot\cdot + Y_5)}\right). \tag{B.23}$$

REFERENCES

1. Vannice, M. A., and Chou, P., "Proceedings, 8th International Congress on Catalysis, Berlin, 1984," Vol. V, p. 99. Dechema, Frankfurt-am-Main, 1984.
2. Chou, P., and Vannice, M. A., *J. Catal.* **107,** 129 (1987).
3. van Meerten, R. Z. C., and Coenen, J. W. E., *J. Catal.* **37,** 37 (1975).
4. Moyes, R. B., and Wells, P. B., "Advances in Catalysis," Vol. 23, p. 121 (1973).
5. Paal, Z., *J. Catal.* **91,** 181 (1985).
6. Hofmann, P., Horn, K., and Bradshaw, A. M., *Surf. Sci.* **105,** L260 (1981).
7. Waddill, G. D., and Kesmodel, L. L., *Phys. Rev. B* **31,** 4940 (1985).
8. (a) Garfunkel, E. L., Maj, J. J., Farias, M. H., Frost, J. E., and Somorjai, G. A., *J. Phys. Chem.* **87,** 3629 (1983); (b) Garfunkel, E. L., Farias, M. H., and Somorjai, G. A., *Amer. Chem. Soc.* **107,** 349 (1985).
9. Tetenyi, P., and Babernics, L., *J. Catal.* **8,** 215 (1967).
10. van Meerten, R. Z. C., Verhaak, A. C. M., and Coenen, J. W. E., *J. Catal.* **44,** 217 (1976).
11. Orozco, J. M., and Webb, G., *Appl. Catal.* **6,** 67 (1983).
12. Selwood, P. W., *J. Amer. Chem. Soc.* **79,** 4637 (1957).
13. Sayers, C. M., and Wright, C. J., *J. Chem. Soc. Faraday Trans. I* **80,** 1217 (1984).
14. Van Meerten, R. Z. C., de Graaf, T. F. M., and Coenen, J. W. E., **46,** 1 (1977).
15. Aben, P. C., van der Eijk, H., and Oelderick, J. M., "Proceedings, 5th International Congress on Catalysis, Palm Beach, 1972" (J. W. Hightower, Ed.), Vol. 2, p. 48. North-Holland, Amsterdam, 1973.
16. Mirodatos, C., *J. Phys. Chem.* **90,** 481, (1986).
17. Bond, G. C., "Catalysis by Metals." Academic Press, New York, 1962.
18. Schwab, G. M., and Pietsch, E., *Z. Physik. Chem.* **81,** 385 (1928).
19. Levy, R. B., and Boudart, M., *J. Catal.* **32,** 304 (1974).
20. Neikam, W. C., and Vannice, M. A., *J. Catal.* **27,** 207 (1972).
21. Neikam, W. C., and Vannice, M. A., "Catalysis" (J. W. Hightower, Ed.), p. 609. North-Holland, Amsterdam, 1973.
22. Nelder, J. A., and Mead, R., *Comput. J.* **7,** 308 (1964).
23. van Meerten, R. Z. C., and Coenen, J. W. E., *J. Catal.* **46,** 13 (1977).
24. Chou, P., Ph.D. thesis, The Pennsylvania State University, 1986.
25. Nyberg, G. L., and Richardson, N. V., *Surf. Sci.* **85,** 335 (1979).
26. Bertolini, J. C., Dalmai-Imelik, G., and Rousseau, J., *Surf. Sci.* **67,** 478 (1977).
27. Lehwald, S., Ibach, H., and Demuth, J. W., *Surf. Sci.* **78,** 577 (1978).
28. Suhrmann, R., "Advances in Catalysis," Vol. 9, p. 88 (1957).
29. Jobic, H., Tomkinson, J., Candy, J. P., Fouilloux, P., and Renouprez, A. J., *Surf. Sci.* **95,** 496 (1980).
30. Silvert, J. A., and Selwood, P. W., *J. Amer. Chem. Soc.* **83,** 1033 (1961).
31. Martin, G. A., and Imelik, B., *Surf. Sci.* **42,** 157 (1974).
32. Garnett, J. L., and Sollich-Baumgartner, W. A., "Advances in Catalysis," Vol. 16, p. 95 (1966).
33. Erkelens, J., and Eggink-du Burck, S. H., *J. Catal.* **15,** 62 (1969).
34. Saunders, P. C., and Hightower, J. W., *J. Phys. Chem.* **74,** 4324 (1970).
35. Sinfelt, J. H., and Rohrer, J. C., *J. Phys. Chem.* **65,** 978 (1961).
36. Rohrer, J. C., Hurwitz, H., and Sinfelt, J. H., *J. Phys. Chem.* **65,** 1458 (1961).
37. Yu, Y. F., Chessick, J. J., and Zettlemoyer, A. C., *J. Phys. Chem.* **63,** 1626 (1959).
38. Pope, C. G., *J. Phys. Chem.* **90,** 835 (1986).

39. Misono, M., Saito, Y., and Yoneda, Y., "Proceedings, 3rd International Congress on Catalysis, Amsterdam, 1964," Vol. 1, p. 408. Wiley, New York, 1965.
40. Primet, M., Garbowski, E., Mathieu, M. V., and Imelik, B., *J. Chem. Soc. Faraday I* **76,** 1953 (1980).
41. Vannice, M. A., Hyun, S. H., Kalpakci, B., and Liauh, W. C., *J. Catal.* **56,** 358 (1979).
42. Chou, P., and Vannice, M. A., *J. Catal.* **104,** 1 (1987).
43. Fouilloux, P., *Appl. Catal.* **8,** 1 (1983).
44. Yoon, K. J., and Vannice, M. A., *J. Catal.* **82,** 457 (1983).
45. Anderson, J. R., and Kemball, C., "Advances in Catalysis," Vol. 9, p. 51 (1957).
46. van Meerten, R. Z. C., Morales, A., Barbier, J., and Maurel, R., *J. Catal.* **58,** 43 (1979).
47. Martin, G. A., and Dalmon, J. A., *J. Catal.* **75,** 233 (1982).
48. Benson, S. W., "Thermochemical Kinetics." Wiley, New York, 1976.
49. Zlotina, N. E., and Kiperman, S. L., *Kinet. Catal.* **8,** 1129 (1967).
50. Badilla-Ohlbaum, R., Neuberg, H. J., Graydon, W. F., and Phillips, M. J., *J. Catal.* **47,** 273 (1977).
51. Boudart, M., and Djega-Mariadassou G., "Kinetics of Heterogeneous Catalytic Reactions." Princeton Univ. Press, Princeton, NJ, 1984.